2024 IEEE/ASME International Conference on Advanced Intelligent Mechatronics (AIM)
July 15-19, 2024. Boston, MA, USA

Characterization of Hip Abduction Exoskeleton for Assistance During Gait Perturbations

Vaibhavsingh Varma, Sujay N. Patel, Nicholas P. Wilson, and Mitja Trkov

Abstract— **Robotic lower limb exoskeletons have been shown to successfully provide joint torques to assist human subjects during walking. Assisting the wearer during gait perturbations to prevent falls still poses a challenge due to specific requirements of the device, and complex bipedal dynamics of recovery. In this study, we present a hip exoskeleton device with pneumatically actuated abduction-adduction motion to provide hip torque for assisting with lateral balance. The device was designed to be wearable, allow integration with previously developed wearable gait perturbation detection system and knee exoskeleton, and produce fast actuation to provide assistive joint torque during gait perturbations. We present the results of the experimental benchtop tests of the device. The maximum torque output and rate of torque development were characterized using a load cell. The maximum angular displacement, with added weights to simulate the leg inertia, was recorded using an inertial measurement unit sensor. Lastly, a preliminary test on a human subject demonstrated that the device, when exerting instantaneous hip abduction torque during swing walking gait, can effectively modify foot placement in the lateral direction. This work contributes towards developing exoskeleton control strategies for assistance during gait perturbations to prevent falls.**

I. INTRODUCTION

Gait disturbances are a common occurrence in elderly adults leading to decreased mobility and falls that reduce the quality of life and increase morbidity and mortality [1]. Higher mortality rates from gait disturbances are primarily due to failure to correct unexpected perturbations in a short amount of time, leading to falls [2]–[4]. Many methods exist to decrease the frequency and severity of fall occurrences, primarily by removing hazards from the area and neuromuscular training. Training in particular is an effective approach, drastically decreasing the number of falls experienced due to perturbation [5], [6]. Repetitive training has been shown to be effective, with a higher training frequency leading to fewer falls [7]. Exoskeleton devices such as human body posturizer have also been used for training to prevent falls with positive results [8].

Robotic exoskeletons can supplement human joints with an assistive torque, which can increase stability by helping to restore normal gait patterns [9]. These devices can assist during the human gait by providing continuous assistance to maintain an upright posture. However, most of these devices and controllers are often not designed to deal with sudden perturbations. In recent years, fast-actuating exoskeleton devices mounted to the knee of the slipping leg [10] or hips [11], [12] have shown promise in providing a proportional flexion or extension torque at necessary time instances to restore the subject's balance. Fast-acting exoskeleton devices attached to the knee of the trailing leg have also shown the ability to immediately force the foot into contact with the ground, assisting with the restoration of the subject's base of support [13]. Recently, the use of knee exoskeleton to provide knee joint torque has been demonstrated to assist during slip balance recovery in the sagittal plane [14]. Unfortunately, most current approaches focus on joint motion in the sagittal plane and therefore are unable to assist with stability in the frontal plane [12].

The step width tends to increase during recovery from slip, particularly in older subjects [15] and exoskeleton assistance for hip abduction could prove helpful. Lateral falls also pose a significant risk to older adults, particularly at the hip area [16], with a study of hip fractures in the elderly reporting 76% of recorded occurrences happening as a result of a sideways fall [17]. Hip abduction-adduction assistance is important for gait stability among the elderly due to the effect of physiological changes on the base of support and margin of stability [18]. Hip abduction assistance has been shown to improve balance-related gait parameters [19]. Researchers have recently developed a hip abduction-adduction assistance exoskeleton [20] and reported step width variations for varying stiffness of admittance controlled hip abduction-adduction exoskeleton without significant effect on gluteus medius muscle while walking [21]. They conclude that this can prove useful for closed-loop control design for mediolateral foot placement. Contrary to traditional exoskeletons, fall safety-oriented devices should provide rapid but momentarily assistance when necessary (i.e., during a loss of balance) and minimally impede the subject's natural walking gait [13].

In this paper, we present a hip exoskeleton device to provide hip abduction assistive torques for lateral leg repositioning during gait perturbations. benchtop characterization of the device was performed to validate its functionality and torque generation capabilities. Experiments using simulated leg inertia were performed to derive a controller for simulated lateral hip actuation. The device and controller were then tested on a human subject during standing to first statically validate device functionality. The system was then validated while walking to demonstrate its effectiveness in lateral leg repositioning during the swing phase. The main contributions of this work include the development of a

This material is based upon work partially supported by the National Science Foundation under Grant No. 2301816. (*Corresponding author: M. Trkov*).

V. Varma, S. N. Patel, N. P. Wilson, and M. Trkov are with the Department of Mechanical Engineering, Rowan University, Glassboro, NJ 08028, USA (email: varmav83@students.rowan.edu; patels39@students.rowan.edu; wilson135@students.rowan.edu; trkov@rowan.edu).

device for lateral leg placement assistance that can be used to aid during lateral balance loss and recovery.

The remainder of the paper is organized as follows. We first present the exoskeleton prototype and benchtop characterization methodology in Section II. Next, we present the experimental results of benchtop testing and human subject testing results in Section III. We conclude with a discussion and summary.

II. MATERIALS AND METHODS

A. Hip Abduction Exoskeleton Prototype

Fig. 1a shows a prototype of the hip abduction device worn by the subject. The exoskeleton consists of three wearable parts that include a hip device, a knee brace, and a backpack that includes an actuation system and electronics. Our previously developed knee brace [13] was integrated with our hip device for completeness of the leg exoskeleton system, however, was not actuated in this study. The tested device was unilateral and was worn only on the right leg. The hip device connects the torso and thigh using a 2-degree-of-freedom (DOF) joint. The hip flexion-extension hinge joint is passive and allows unconstrained leg motion in a sagittal plane. The hip abduction joint is actuated using a pneumatic cylinder (SC40X75, CHLED). Bowden tube and steel cable is used to transfer the force from the cylinder to the mechanism with a 100 mm long moment arm connected to a ϕ12.7 mm keyed steel shaft to exert an assistive hip torque. Using a Bowden cable system has the advantage of arbitrarily positioning the air cylinder at the back rather than attaching it to the limb thus reducing the inertia of the exoskeleton at the limbs and minimizing effects on the walking gait. The mechanism at its extreme positions is shown in Fig. 1b. The air cylinder is pressurized by either a 12g CO2 cartridge when the subject wears it or a stationary high-pressure source for bench testing. The rest of the device components were primarily constructed from machined 6061 aluminum and 3D-printed parts from polylactic acid (PLA) material. The actuators and electronics were mounted on support at the back of the wearer, high enough to allow for sitting. The current design incorporates an independent passive hip-flexion joint in series after the abduction mechanism, therefore avoiding interference between the two movements. When the device is not actuated, the bending of the portion of the steel cable between the actuation arm and the mechanical stop allows for unconstrained motion in the frontal plane. The device allows maximum hip abduction of 45 degrees to guarantee the safety of the subjects which is enforced by a maximum movement of the moment arm before hitting a hard stop as well as by the maximum stroke of the cylinder.

Fig. 2 shows the schematics of electronics, exoskeleton device, and experimental setup. The electro-mechanical-pneumatic parts include a 14.4 V 4S 5200 mAh LiPo battery to power the actuation circuit, the air cylinder, a solenoid valve, a relay control circuit, a microcontroller (Arduino NANO), and pressure regulators with the cartridge. The cylinder is controlled by a 5-port 3-way center stable solenoid valve, powered through 12 V relays. The relay, in turn, is controlled by the microcontroller which opens and automatically closes the solenoid valve. All electrical devices are powered through the same battery pack. Pressure is supplied from a pressure source or cartridge that can be easily switched out, and regulated between 20 and 50 psi.

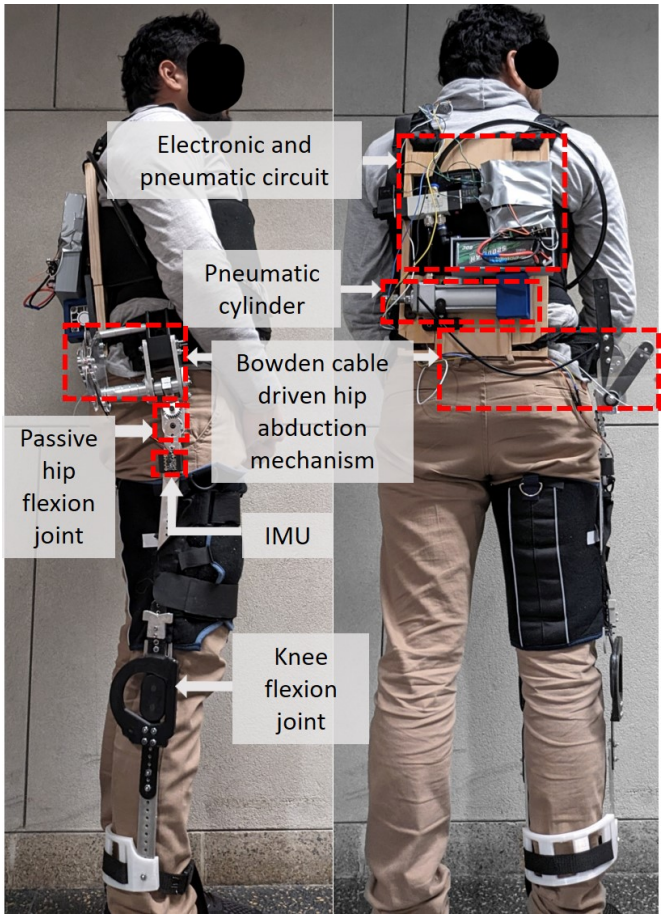

(a)

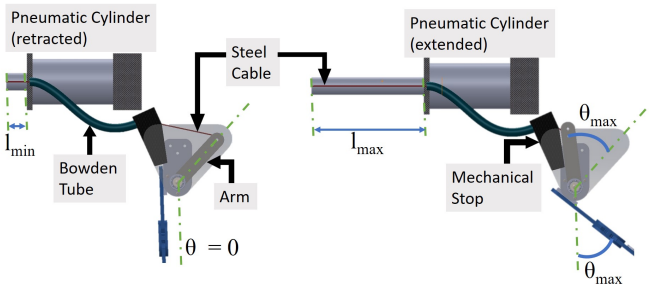

(b)

Figure 1: Hip abduction exoskeleton prototype. (a) Side view showing integrated hip and knee device (left). Back view showing actuators and electronics (right). (b) Back view of hip abduction mechanism model showing fully retraced cylinder when in standing position (left) and fully extended cylinder during abducted leg position (right).

B. Benchtop Testing

We first performed bench testing to characterize the device to evaluate its torque generation capabilities and guarantee safe operation before testing it on a human subject.

1) Torque Output: The benchtop tests included measurements of the maximum torque and rate of torque development under various pressure inputs and duration of pressure supply. Prior to testing, we integrated the hip exoskeleton with a knee device and considered a fully extended (leg) position to account for maximum moments of inertia and masses of the whole hip-knee exoskeleton device that is required to assist with the fall prevention strategy in both sagittal and lateral planes. Any contraction of the knee or flexion/extension of the hip would reduce the moment of inertia of the device and body when worn, however, this is constrained due to centrifugally acting forces during actuation.

During the benchtop testing, the hip attachment was rigidly fixed and an S-load cell was placed at the tip of the device at the shank attachment to measure the exerted force (see Fig. 2). The force measurements were used to compute the generated hip abduction torque. The cylinder actuation was timed by the microcontroller and each trial consisted of eight loading cycles, 3 trials were repeated at each pressure level from 20-50 psi with increments of 10 psi. The load cell data was recorded at a 10 Hz sampling frequency. The pressure was varied and torque was calculated from the peak load cell readings ($F_{loadcell}$) and moment arm length (L), i.e., distance from the shaft center to the load cell attachment point, calculated as $T = F_{loadcell}L$.

2) Range of Motion: For testing the range of abduction motion under various applied pressures and duration of solenoid activation, we simulated realistic conditions by using a 12 kg weight added in the brace simulating the mass and inertia of a leg based on empirical relations [22]. The range of motion depends on the stroke of the cylinder, hence the stroke was varied at each pressure level by timing the solenoid valve activation for 50, 75, and 100 ms, respectively, at each pressure level. Each trial consisted of two actuation cycles and corresponded to a combination of pressure and activation time out of the possible 12 combinations. Three trials were repeated for each combination. An IMU sensor (Adafruit BNO055) placed at the thigh of the exoskeleton was used to output and record the absolute angle displacement. The IMU was first calibrated in the initial free-hanging position of the exoskeleton. The data was collected at a rate of 10 Hz.

C. Human Subject Testing

1) Standing Perturbations: After performing the bench testing and validating the device performance of available torque, range of motion, and safe operation, we proceeded to conduct tests with a human subject (male, 29 years, 70 kg body weight). The subject wore the exoskeleton and all points of contact were secured to a tight at a comfortable level as per the subject's feedback. For the first test configuration, the subject wore the exoskeleton as shown in Fig. 1 and stood with the free leg (one the without exoskeleton) planted on a raised wooden platform, while the leg wearing the exoskeleton was hanging in the air. The exoskeleton was then actuated at 50 psi for 100 msec of the solenoid valve activation time to get a maximum range of motion and held in position for 3 seconds before being released. Five actuation cycles were repeated for each trial. The safety of the subject was ensured by appropriate support from structural members and the presence of two testers. Five trials were conducted and the hip abduction range of motion was recorded using an IMU placed on the thigh brace of the exoskeleton attached to the subject's leg.

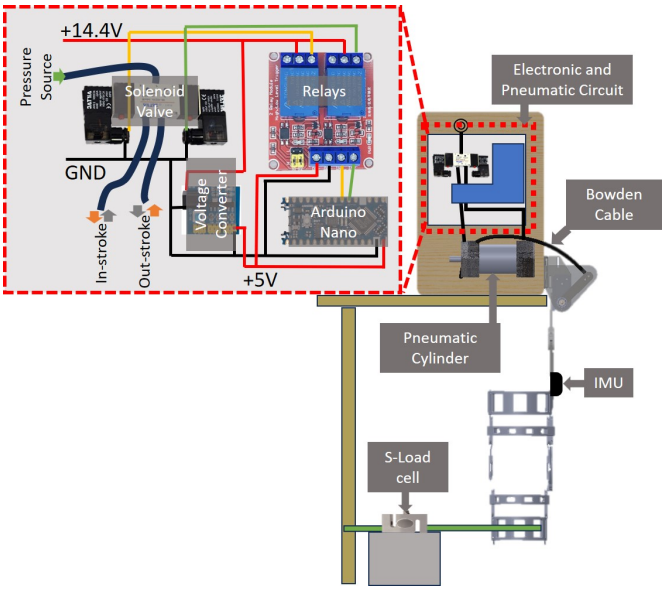

Figure 2: Experimental setup for bench testing the hip abducting exoskeleton.

2) Walking Perturbation: After the standing tests limb lengths were measured. The subject was asked to walk with the exoskeleton for 3 minutes to get familiar walking with the exoskeleton and to let the braces settle on the body. Then the subject was asked to walk at a self-selected speed in a straight line and the exoskeleton was actuated during the third consecutive step with that leg from the start to allow reaching a steady gait. The IMU was used to record the angular displacements during walking and perturbation of the leg. The study was approved by the Rowan University's institutional review board.

III. EXPERIMENTAL RESULTS

A. Benchtop Testing Results

1) Torque Output: The torque output of the prototype is presented in Fig. 3. Peak torque was reached at approximately 0.28 sec after actuation for all pressures. Fig. 3a shows the average torque increment at each pressure level from the time of actuation (0 sec) to the time when peak load cell reading was reached which corresponds to peak torque application. The mean applied torque increased with pressure as expected (see Fig. 3b). Torque increases from 8.2 N-m at 20 psi to 24.7 N-m at 50 psi. The rate of torque

development is shown in Fig. 3c. Maximum rate of torque development was 91 ± 12.2 Nm/s at air pressure of 50 psi. Together, these characteristics are significant for controlling the actuator based on an individual's physiology as well as the type of movement required. The requirements of motion after a perturbation can vary based on its severity. Using these characteristics it may be possible to generate different actuator control signals at different stages during recovery from the perturbation. Both the magnitude and rate of torque applied may be controlled for optimal recovery motion.

2) Range of Motion: The changes in the range of motion of the hip exoskeleton with respect to supplied air pressure and duration of application are shown in Fig. 4. As expected, the range of motion increases with the increase in applied pressure. However, the time of application of pressure (i.e., the time of solenoid activation) was observed to control the stroke of the cylinder. Therefore, the time of solenoid activation has also been considered a significant factor for controlling the range of motion. 50 msec was considered as the minimum duration for solenoid activation as the cylinder motion was not significant below this timing whereas full stroke was achieved at 100 msec and 50 psi pressure.

It is clear from Fig. 4 that there is a significant effect of solenoid activation time on the abduction angle achieved. Therefore, activation timing is an important parameter that may be used to control the movement during perturbations. By varying these timings it will be possible to move the leg by a desired angle during a perturbation for optimal recovery. Thus a combination of pressure and activation time provides control over both the torque applied and the range of motion achieved. Therefore, successful perturbation recovery controllers can be developed given the kinematic and dynamic requirements for recovery.

B. Human Subject Testing Results

1) Standing Activation: Fig. 5 show the mean angular displacements for five trials of the human subject experiments while subject was wearing the exoskeleton in a standing configuration. The results show that the overall mean angular displacement across all trials is approximately 11.8 deg at 50 psi of pressure supply. The highest mean of maximum abduction angle in a single trial was 13 deg and it was only observed in the first trial. Compared to the mean abduction angle achieved during benchtop tests at same condition of applied 50 psi pressure and 100 msec activation time of the solenoid, the values from human subject tests are lower. The reduction in the range of motion can be attributed to many reasons including the compliant nature of the human body and the resistance of the human leg to movement. The compliance at the human-exoskeleton interfaces causes the loss of full range of motion as some of the movement is lost due to deformation of the tissue/body. The deformation of the subject's body was evident at the hip-thigh brace because it is not feasible to rigidly attach the exoskeleton to the body even after securing the braces tightly to the body, due to inherently soft tissue properties. It is also not entirely possible for the subject to hold the exoskeleton leg in a dead hanging position

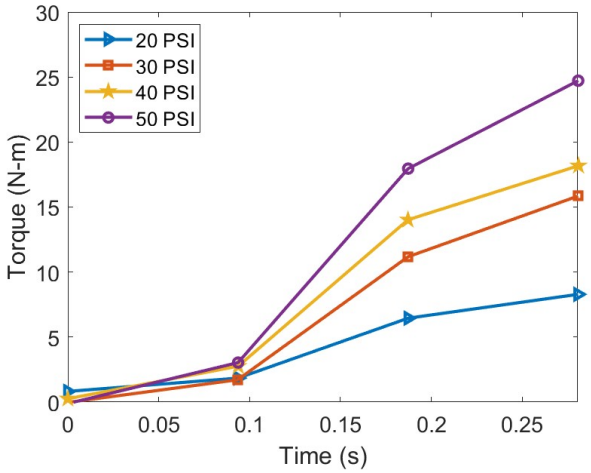

(a)

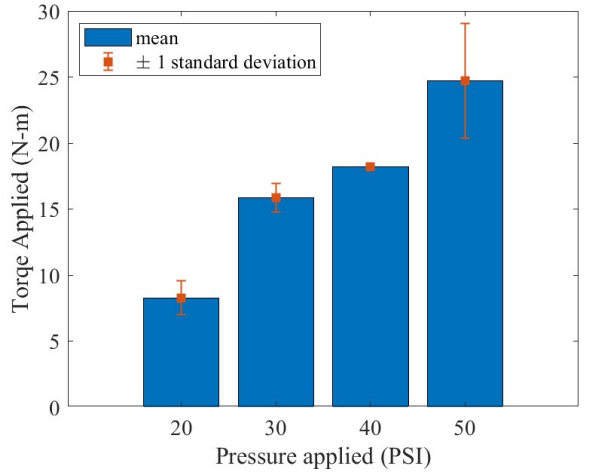

(b)

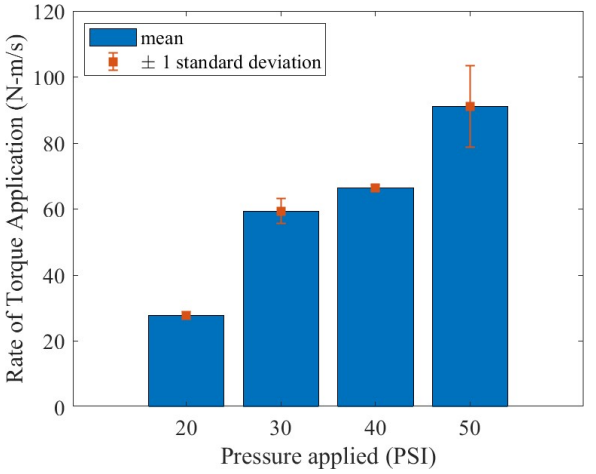

(c)

Figure 3: (a) Average torque application profiles at each pressure. (b) Mean torque developed at each pressure with ± 1 standard deviation range over considered trials. (c) Mean rate of torque development with ± 1 standard deviation range over considered trials.

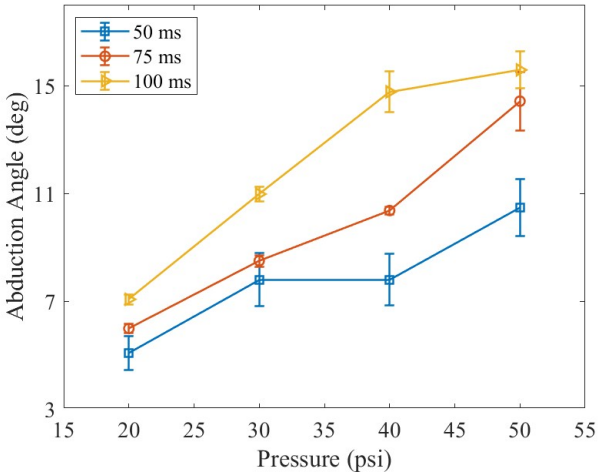

Figure 4: Mean abduction range of motion for applied pressures of 20-50 psi and solenoid activation timings of 50, 75, and 100 ms.

thus developing some resistance to the movement caused by the exoskeleton actuation. This resistance corresponds to the concept of joint impedance [23] which can be considered an important parameter to explore for estimating the amount of assistance required in different situations.

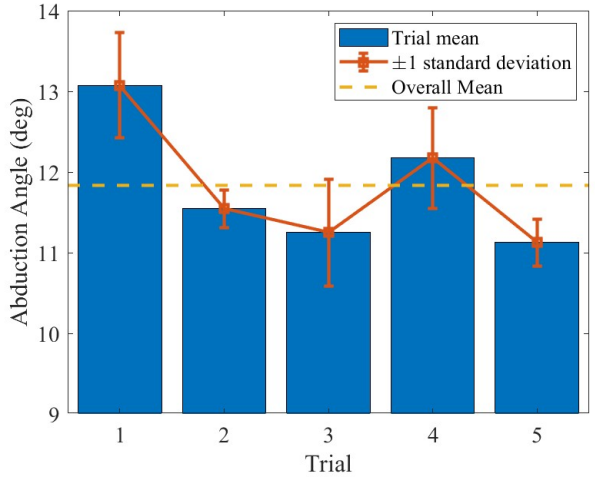

Figure 5: Results of mean ±1 standard deviation of abduction angle achieved in each trial of human subject experiments during standing tests.

2) Walking Perturbation: After the standing trials, the subject was instructed to walk with the exoskeleton and was given a perturbation by the exoskeleton. The profiles of hip abduction-adduction angle observed during five such walking trials are presented in Fig. 6a. The perturbation occurred after the toe-off of the third step. The exoskeleton controller was programmed to actuate the cylinder randomly during the third swing phase after the start of the walking trial as this corresponded with the beginning of the third step based on the observed normal walking speed and profile of the subject. The angular displacement in a lateral direction significantly increased shortly after the exoskeleton was actuated. This confirms the action of the exoskeleton in affecting the hip joint motion in the frontal plane. The average peak angles achieved in normal walking steps while wearing the (unactuated) exoskeleton are significantly lower than the average peak angles when perturbed by the exoskeleton as shown in Fig. 6b. The difference is approximately 14 deg. The exoskeleton can thus be considered effective for the task of instantaneous lateral leg repositioning.

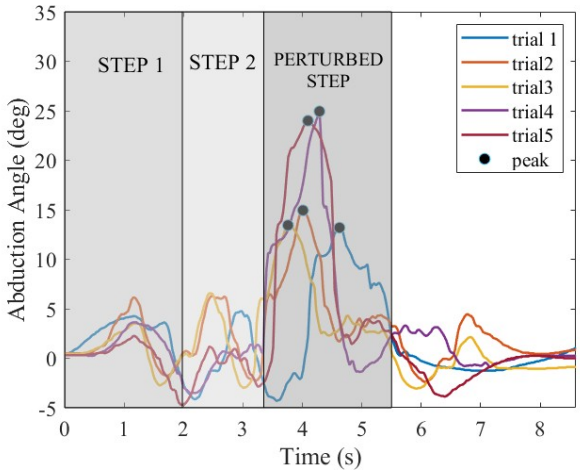

(a)

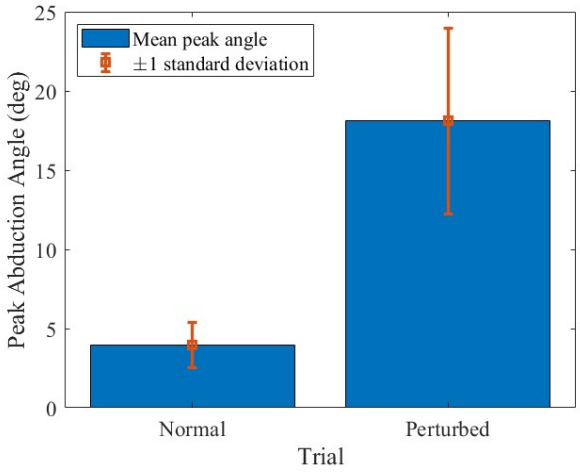

(b)

Figure 6: (a) Variation of hip abduction angle while walking with exoskeleton with activation during the swing portion of the third step after the start of walking. Torque is applied from the start of the perturbed step for 0.5 sec to reach the peak angle for each trial. (b) Comparison of peak angles for normal steps and perturbed step for each trial.

IV. CONCLUSIONS AND FUTURE WORK

In this work, we presented an extension of the design of an existing cable-driven knee exoskeleton by incorporating the active hip abduction-adduction joint. First, the device was characterized by conducting benchtop tests. In our tests, we used a load cell to confirm the expected behavior of

different pressure supply levels on increasing the applied torque at the hip joint. Further, the exoskeleton was loaded with dead weight, simulating leg mass, and actuated at different pressure levels with three different solenoid valve actuation times. The results of these tests proved that the range of motion of the exoskeleton could be controlled using a combination of pressure and actuation times of the solenoid valve. After the benchtop tests, human subject trials were conducted to prove the effectiveness of the exoskeleton design in repositioning the human leg while standing and walking. The exoskeleton was able to move the free-hanging human leg by 11.8 deg on average when the subject was standing on the non-actuated leg. This deflection was less than that observed in benchtop tests under same applied pressure conditions, possibly due to the compliance of the human body and joint impedance. Additionally, walking trials confirmed that the exoskeleton is capable of providing active perturbation/assistance to the leg while in motion. An average deflection of 18 deg was observed while walking. The current design can be improved by redesigning the interfaces to fit multiple subjects. The prototype can fit individuals in a height range of 1.70 to 1.75 m which could be increased in future iterations. The backpack can be improved to incorporate more actuators for other degrees of freedom. The simultaneous operation of hip and knee joints was out of the scope of this study; however, assisting both sagittal and frontal planes is required for holistic recovery from perturbations to prevent falls.

In conclusion, this work on hip abduction exoskeleton underscores the possibility of affecting hip joint motion in the frontal plane. Very few exoskeleton designs have addressed the frontal plane motion of lower limbs and this study characterizes a novel hip abduction-exoskeleton design. Recovery from perturbations such as slips and trips may require an assistive device to have actuated movement in the frontal plane for successful recovery. Therefore this work contributes toward laying a foundation for future investigations aimed at the development of assistive devices and control strategies for lower limb joints including hip abduction-adduction for recovery from gait perturbations.

V. ACKNOWLEDGEMENTS

The authors would like to thank students K. Z. Uddin, A. K. Singh, and A. Khalili from Rowan University for their help with the preparation and conducting the experiments.

REFERENCES

[1] K. Jahn, A. Zwergal, and R. Schniepp, "Gait disturbances in old age: classification, diagnosis, and treatment from a neurological perspective," *Deutsches Ärzteblatt International*, vol. 107, no. 17, p. 306, 2010.

[2] W. Berg, H. Alessio, E. Mills, and C. Tong, "Circumstances and consequences of falls in independent community-dwelling older adults," *Age and Ageing*, vol. 26, Jul. 1997.

[3] T. Masud and R. Morris, "Epidemiology of falls," *Age and Ageing*, vol. 30, Nov. 2001.

[4] A. Ambrose, G. Paul, and J. Hausdorff, "Risk factors for falls among older adults: a review of the literature," *Maturitas. 2013 May;75(1):51-61. doi:*, vol. 75, no. 1, pp. 51–61, 2013.

[5] K. Bieryla and M. Madigan, "Proof of concept for perturbation-based balance training in older adults at a high risk for falls," *Arch. Phys. Med. Rehabil.*, vol. 92, no. 5, pp. 841–843, 2011.

[6] M. Nevisipour, M. Grabiner, and C. Honeycutt, "A single session of trip-specific training modifies trunk control following treadmill induced balance perturbations in stroke survivors," *Gait Posture*, vol. 70, pp. 222–228, 2019.

[7] T. Bhatt, F. Yang, and Y. Pai, "Learning to resist gait-slip falls: long-term retention in community-dwelling older adults," *Arch. Phys. Med. Rehabil.*, vol. 93, no. 4, pp. 557–564, 2012.

[8] W. Verrusio, V. Gianturco, M. Cacciafesta, V. Marigliano, G. Troisi, and M. Ripani, "Fall prevention in the young old using an exoskeleton human body posturizer: a randomized controlled trial," vol. 29, pp. 207–214, 2017.

[9] B. Chen, B. Zi, L. Qin, and Q. Pan, "State of the art research in robotic hip exoskeletons: a general review," *Journal of Orthopaedic Translation*, vol. 20, pp. 4–13, 2020.

[10] M. Trkov, S. Wu, K. Chen, J. Yi, T. Liu, and Q. Zhao, "Design of a robotic knee assistive device (rokad) for slip-induced fall prevention during walking," vol. 50, no. 1. Elsevier, 2017, pp. 9802–9807.

[11] V. Monaco, P. Tropea, and F. e. a. Aprigliano, "An ecologically-controlled exoskeleton can improve balance recovery after slippage," *Sci. Rep.*, vol. 7, no. 46721, 2017.

[12] F. Aprigliano, V. Monaco, P. Tropea, D. Martelli, N. Vitiello, and S. Micera, "Effectiveness of a robot-mediated strategy while counteracting multidirectional slippages," *Robotica*, vol. 37, no. 12, pp. 2119–2131, 2019.

[13] M. Mioskowska, D. Stevenson, M. Onu, and M. Trkov, "Compressed gas actuated knee assistive exoskeleton for slip-induced fall prevention during human walking," in *2020 IEEE/ASME International Conference on Advanced Intelligent Mechatronics (AIM)*, 2020, pp. 735–740.

[14] C. Zhu and J. Yi, "Knee exoskeleton-enabled balance control of human walking gait with unexpected foot slip," *IEEE Robotics and Automation Letters*, 2023.

[15] X. Ren, C. Lutter, M. Kebbach, S. Bruhn, R. Bader, and T. Tischer, "Lower extremity joint compensatory effects during the first recovery step following slipping and stumbling perturbations in young and older subjects." *BMC geriatrics*, vol. 22, p. 656, Aug 2022.

[16] W. Hayes, E. Myers, J. Morris, T. Gerhart, H. Yett, and L. Lipsitz, "Impact near the hip dominates fracture risk in elderly nursing home residents who fall," *Calcif. Tissue Int.*, vol. 52, pp. 192–198, 1993.

[17] J. Parkkari, P. Kannus, M. Palvanen, A. Natri, J. Vainio, H. Aho, I. Vuori, and M. Järvinen, "Majority of hip fractures occur as a result of a fall and impact on the greater trochanter of the femur: a prospective controlled hip fracture study with 206 consecutive patients," *Calcif Tissue Int*, vol. 65, pp. 183–187, 1999.

[18] T. Burton, É. Séguin, and M. Doumit, "Study of hip exoskeleton technology for elderly stability during walking," in *2022 World Automation Congress (WAC)*, 2022, pp. 596–601.

[19] J. Park, K. Nam, J. Yun, J. Moon, J. Ryu, S. Park, S. Yang, A. Nasirzadeh, W. Nam, S. Ramadurai, M. Kim, and G. Lee, "Effect of hip abduction assistance on metabolic cost and balance during human walking," *Science Robotics*, vol. 8, no. 83, p. eade0876, 2023. [Online]. Available: https://www.science.org/doi/abs/10.1126/scirobotics.ade0876

[20] V. Nalam, A. Alili, A. Fleming, X. Tu, M. Liu, and H. Huang, "Development of a hip abduction-adduction exoskeleton for mediolateral assistance," Mar. 2024. [Online]. Available: http://dx.doi.org/10.36227/techrxiv.171171958.81255425/v1

[21] A. Alili, A. Fleming, V. Nalam, M. Liu, J. Dean, and H. Huang, "Abduction/adduction assistance from powered hip exoskeleton enables modulation of user step width during walking," *IEEE Transactions on Biomedical Engineering*, vol. 71, no. 1, pp. 334–342, 2024.

[22] *Anthropometry*. John Wiley & Sons, Ltd, 2009, ch. 4, pp. 82–106. [Online]. Available: https://onlinelibrary.wiley.com/doi/abs/10.1002/9780470549148.ch4

[23] H. van der Kooij, S. S. Fricke, R. C. v. Veld, A. V. Prieto, A. Q. L. Keemink, A. C. Schouten, and E. H. F. van Asseldonk, "Identification of hip and knee joint impedance during the swing phase of walking," *IEEE Transactions on Neural Systems and Rehabilitation Engineering*, vol. 30, p. 1203–1212, 2022. [Online]. Available: http://dx.doi.org/10.1109/TNSRE.2022.3172497